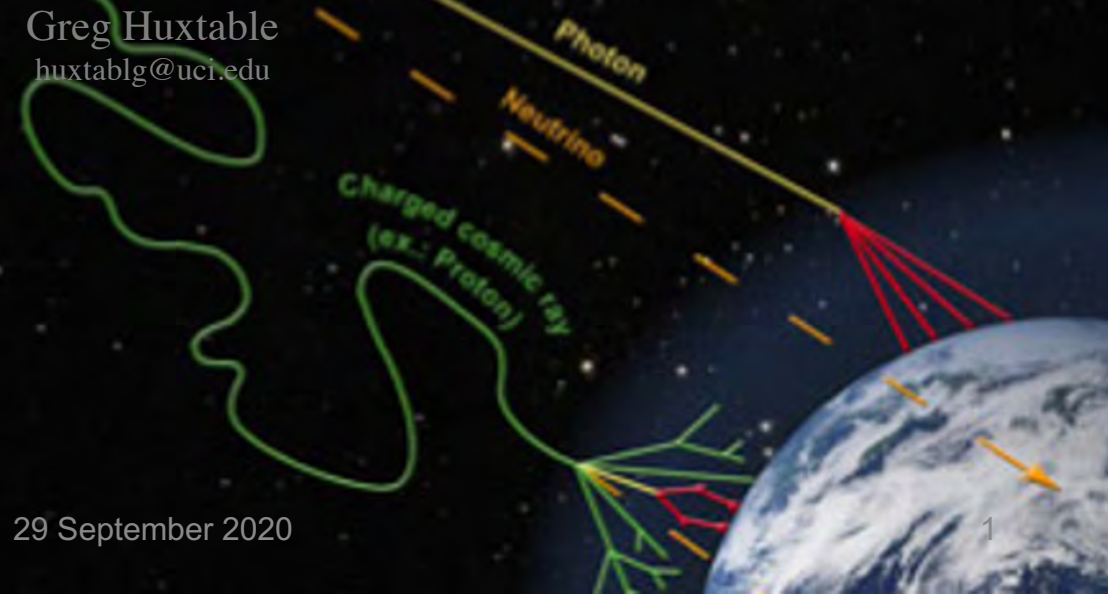
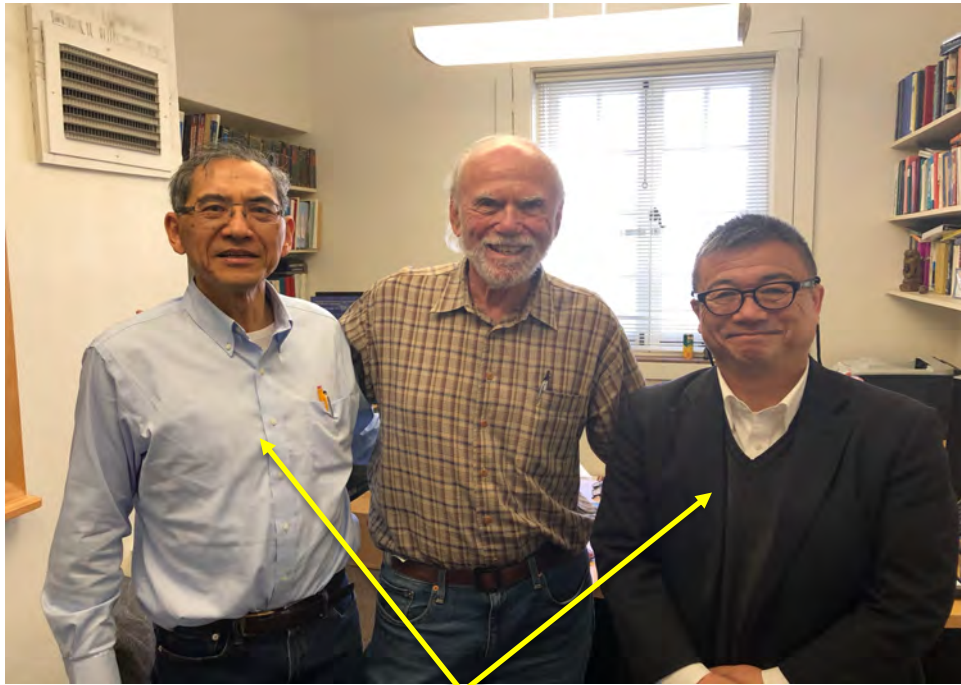


Astrophysical Evidence of Wakefield Acceleration in Galactic and Extragalactic Jets via Gamma Rays and UHECRs

Greg Huxtable
huxtableg@uci.edu



This project was a team effort between members from UCI and UCR, as well as Prof. Toshikazu Ebisuzaki (RIKEN, Japan)



With guidance from both Professor Toshi's we were able to write a nice paper
(submitted to ApJ)

**Astrophysical Evidence of Wakefield Acceleration in Galactic and Extragalactic Jets
via Gamma Rays and UHECRs**

GREGORY B. HUXTABLE,¹ NOOR ELTAWIL,¹ WEI-XIANG FENG,² WENHAO WANG,¹
GABRIEL PLAYER,¹ TOSHIKI TAJIMA,¹ AND TOSHIKAZU EBISUZAKI³

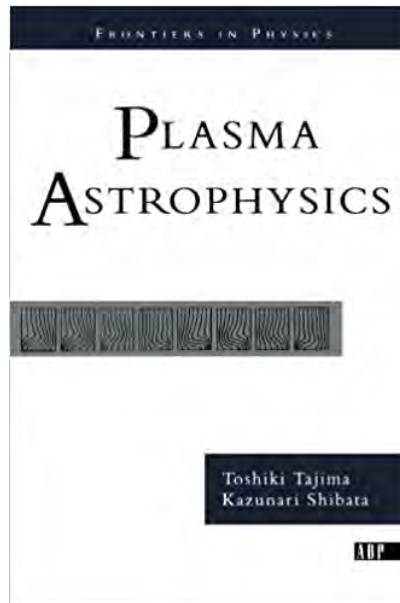
¹*UC Irvine, Physics and Astronomy*

²*UC Riverside, Physics and Astronomy*

³*Computational Astrophysics Laboratory, RIKEN*

PHYS 249 Special Topics: Plasma Astrophysics

In spite of the current pandemic, inter-UC-campus classmates of PHYS 249 were able to complete a very fruitful term project that blossomed into the current version of the paper



Thank you UCI and Overleaf, which made group editing much easier than it would have been 👍

Wakefield

- Inspired by the previous works of Tajima, Dawson, Ebisuzaki, Shibata, Takahashi, and Wheeler, we decided to survey **several very different astrophysical objects** we believe are great candidates for exhibiting signs of WFA in their jets

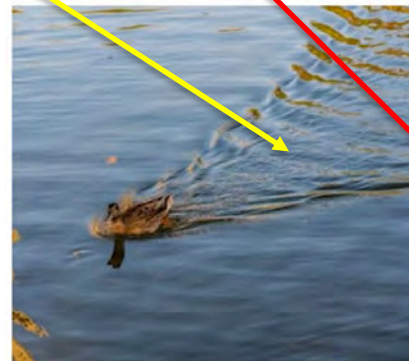
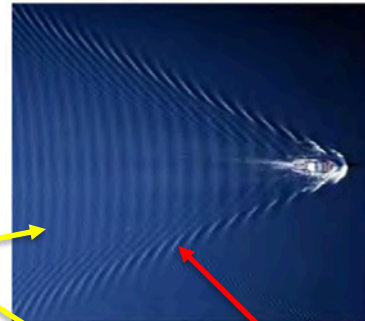
- T. Tajima and Dawson 1979, PhRvL, 43, 267
- T. Tajima and T. Ebisuzaki 2014, Astroparticle Physics, 56, 9
- T. Tajima et al 2020, Rev. Modern Plasma Phys., 4, 7
- Tajima and Shibata, *Plasma Astrophysics*, 1979
- Takahashi et al 2000, Relativistic Lasers and High Energy Astrophysics, 171

Turbulent, $v_{ph} \sim v_T$

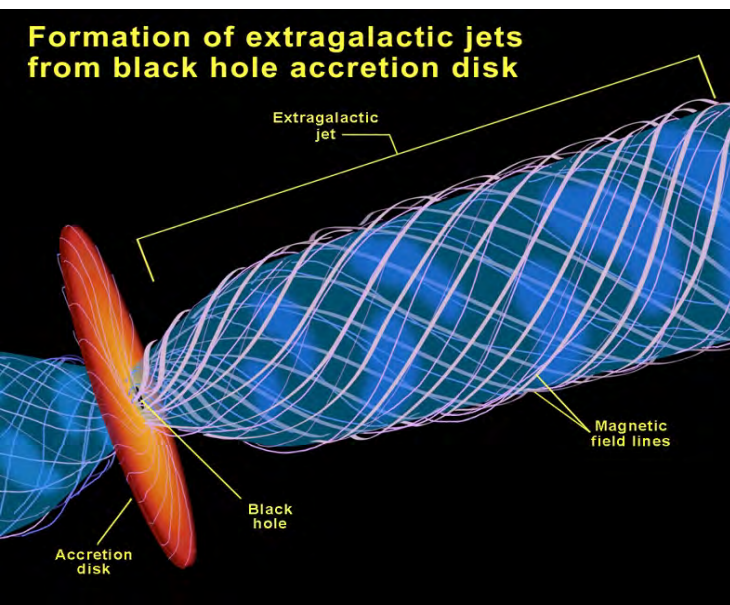


vs

Coherent, $v_{ph} \gg v_T$

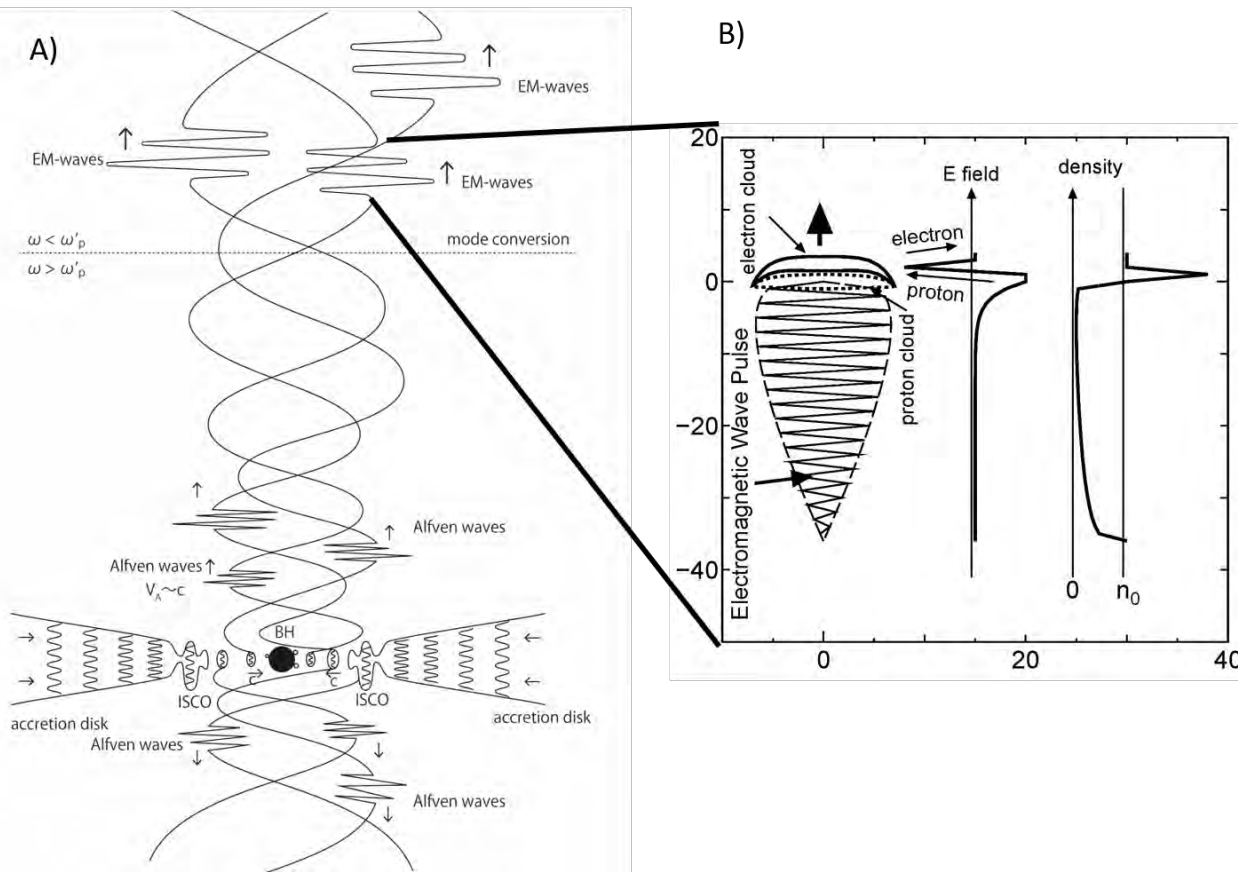


Gulls conserve energy by amplifying the bow wake created by the bird in front of them



WFA in Jets

Plasma at the base of the jet is in the over-dense state $\omega < \omega_p, \omega_c$. Eruptive accretions create Alfvén waves in the base of the jet. Intense Alfvén waves eventually become intense EM waves as $\omega_p \rightarrow \omega$, and $V_A \rightarrow c$.



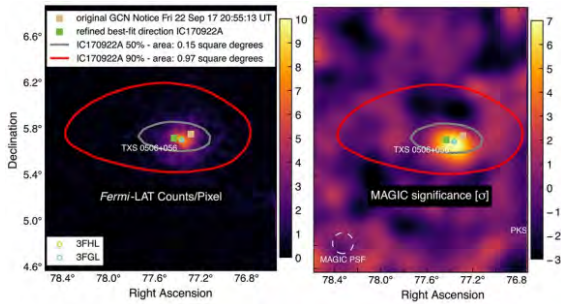
$a_0 \approx 10^{6-10}$ (extremely high compared to laboratory plasmas)
 $n_e \approx 10^4$ (near BH); 10^1 cm^{-3} (along jet, away from BH)
 $D \approx 10^{11-19} \text{ cm}$ (acceleration length)

Jets

- Jets of various sizes are known to exist throughout the universe, likely forming whenever there is an accretion disk and a central object
- Velocity of jet scales with magnetic strength of object, $V_{jet} \propto B$
 - explains why blazars are so much more powerful than smaller microquasars

TXS 0506+056 (blazar)

Telescope. Liverpool, IceCube Collaboration. Science 361, 6398 (2018)

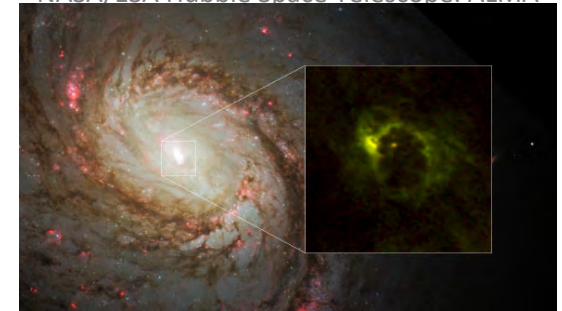


Cen A

© 2016 Cherenkov Telescope Array Observatory gGmbH

NGC 1068

NASA/ESA Hubble Space Telescope. ALMA



M82

NASA/JPL-Caltech/STScI/CXC/UofA/ESA/AURA/JHU



SS 433

NRAO/AUI/NSF, K. Golap, M. Goss; NASA's Wide Field Survey Explorer (WISE)



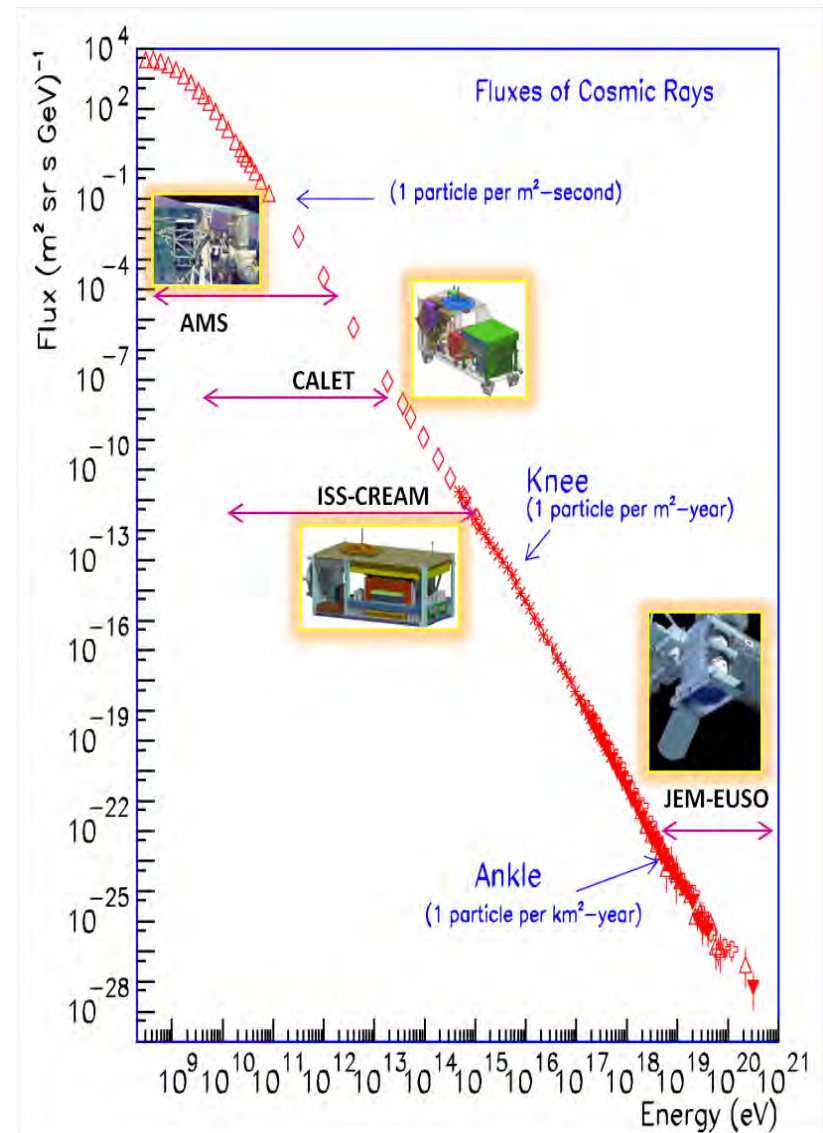
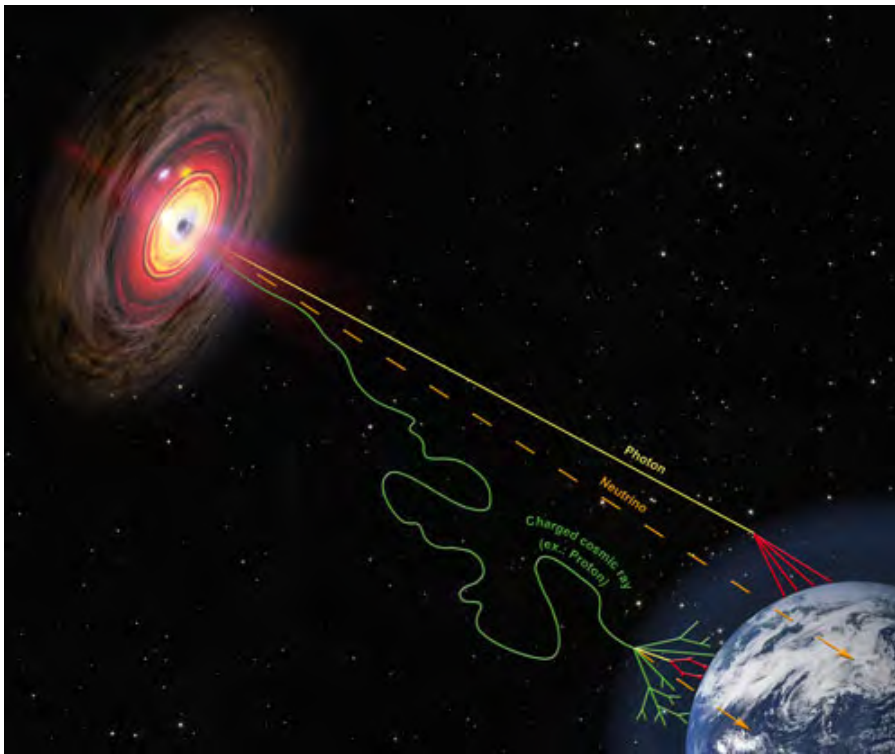
NGC 0253

ESO VISTA Telescope at Paranal Observatory In Chile



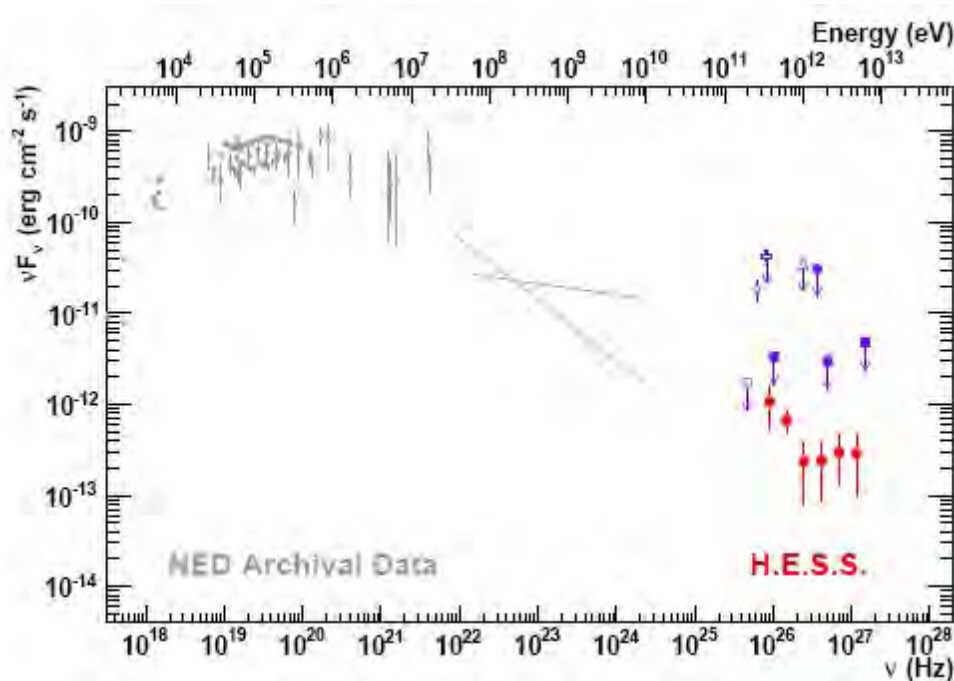
UHECRs

- How ultra high energy cosmic rays (UHECRs) $> 10^{19}$ GeV are accelerated up to such high energies is insufficiently understood by the Physics & Astronomy community
- WFA can easily generate these signals
 - Fermi acceleration cannot



UHE Gamma Rays

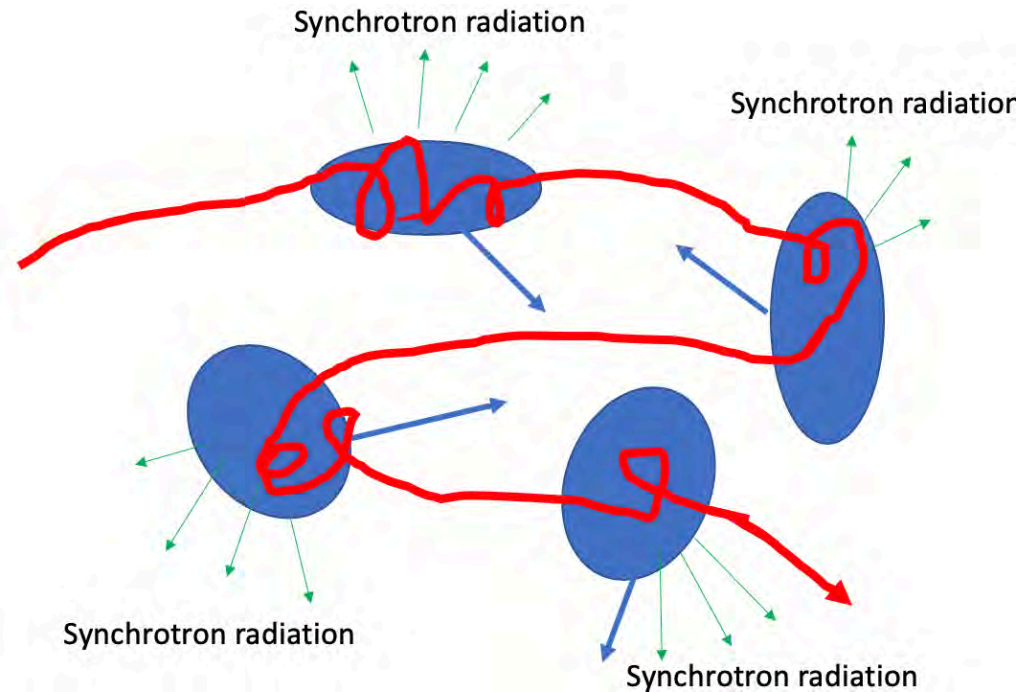
- Similarly, UHE gamma rays ≥ 10 GeV are a mystery from the perspective of Fermi acceleration
- Upon reaching the end of the jet, UHE electrons collide with decelerated matter in the “lobes” to produce UHE gamma rays
- Neutrino’s created by collisions of UHE protons/nuclei in the lobes, follow a path parallel to the jet axis since that is the direction of momentum for the collision
 - Leading to gamma ray burst and neutrino burst temporal correlations



Fermi Acceleration

Explains the creation of low E gamma rays, x-rays, microwaves, etc, but fails to explain dynamics in the UHE regime

- Stochastic
- Incoherent
- No time or spatial structure; steady state
- Suffers from large synchrotron loss ($< 10^{19}$ eV)
 - Very difficult for e^- to reach > 10 GeV



Power radiated from bending relativistic charge (J. D. Jackson, 1975)

$$P(t') = \frac{2 e^2 v^4}{3 r^2 c^3} \gamma^4$$

Outline

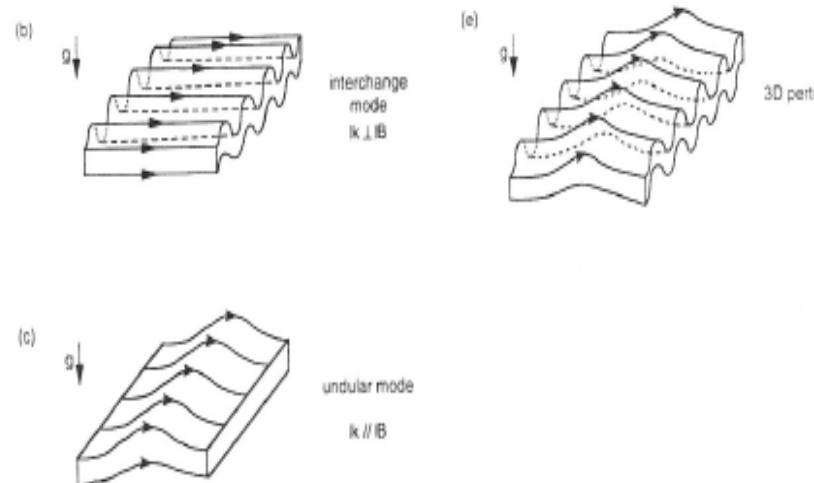
1. Physics of the Accretion Disk
2. WFA in the jet
3. Results
4. Additional Evidence
5. Summary

Accretion & Relevant Instabilities

- Scientists have known for a long time that there must be some mechanism causing matter to lose angular momentum and accrete onto the central engine
 - Eventually to be expelled into the jets
- Beginning with the physics of astrophysical plasmas, we first must understand the relevant instabilities of these systems
 - Parker instability
 - Magneto-rotational instability (MRI)
 - Both instabilities are interestingly stabilized by the magnetic tension force
- MRI + Magnetic buoyancy + conservation of angular momentum -> accretion

Parker Instability

- Related to Rayleigh-Taylor and ballooning instability
 - Driven by pressure gradients
- Exponential instability, $A \propto e^t$
- We are always likely going to have thermal convection in these high beta astrophysical plasmas, which generates fluctuations in the magnetic field
 - Also fair to assume flux tubes exist (convective collapse)
- Waves/perturbations in flux tubes can trigger Parker instability; locally intense B field creates a pocket of low density that rises against gravity (magnetic buoyancy)
 - Buoyancy force becomes stronger than magnetic tension $\Delta\rho g > B^2/4\pi r$
 - And is increasingly accelerated by plasma rushing out of the way along the field lines from gravitational free fall
 - Physically similar to the ballooning instability
- Instability speeds increase with flux tube size (Tajima & Shibata 2002)
- Unstable for $\lambda > 9H$, where $H = T/Mg$ is locale pressure scale height

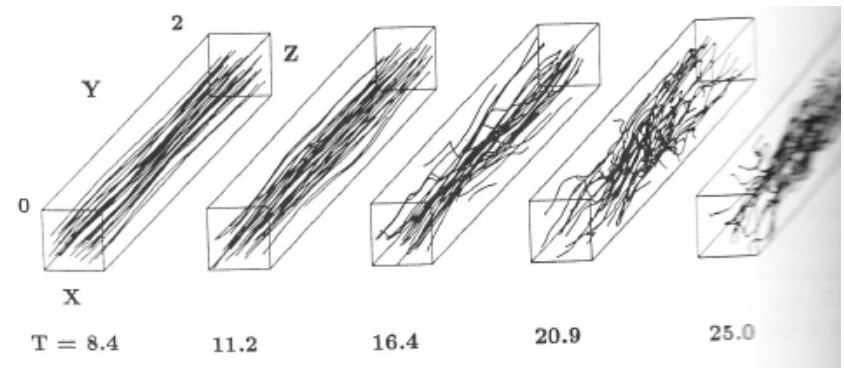
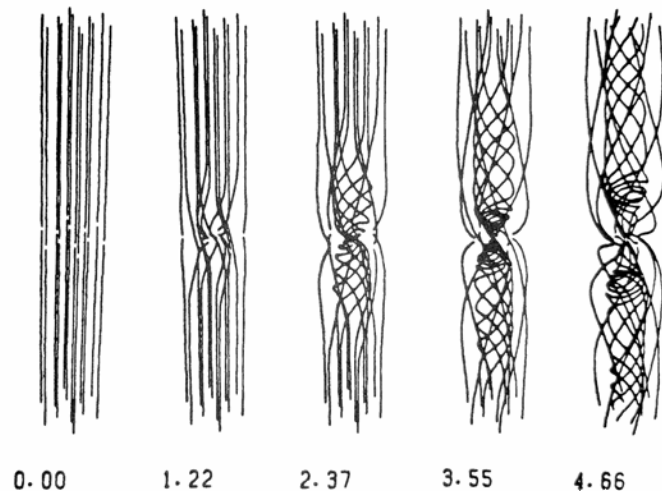


MRI

Differential/Keplerian rotation ($\Omega \propto r^{-3/2}$) twists the magnetic field more and more with time, increasing resistivity, allowing gravity to eventually overcome centrifugal force, leading to “eruptions”.

- stochastic perturbations of fluid elements cause vertical field lines to begin to twist and trigger the MRI
- Occurs even with very weak B-field strengths

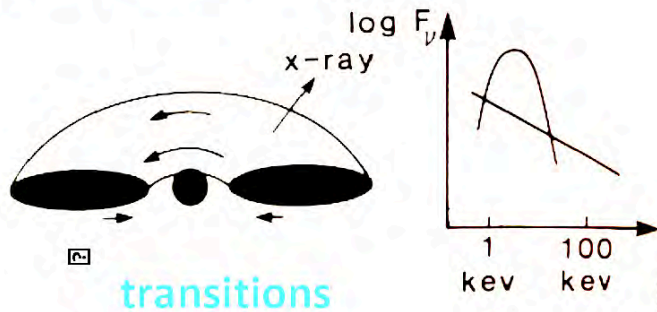
- Creates anomalous viscosity, which leads to transport
- Accretion disk transitions between high beta (soft x-rays) and low beta states (hard x-rays)
- Explains fluctuations in spectral index
- Anomalous resistivity $\eta \sim \delta B^2$, magnetic viscosity $\alpha_B \sim (\delta V_A/C_s)^2$



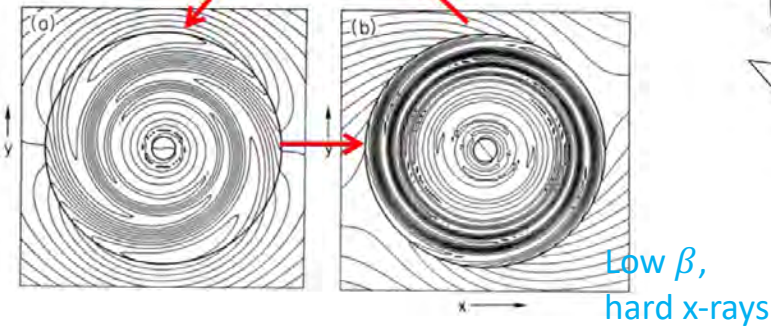
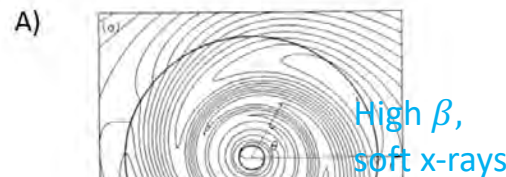
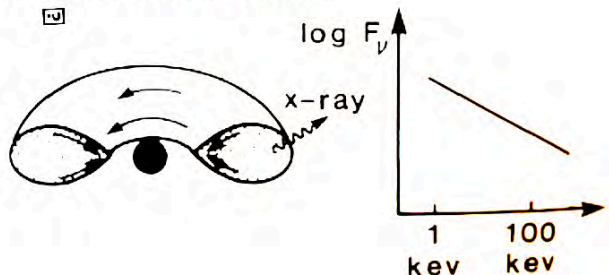
MRI

- Net force on perturbed fluid element $F = \left(\frac{B^2}{4\pi(\lambda/2\pi)^2} - \rho\Omega^2 \right) \Delta r$
- Critical wavelength $\lambda/2\pi > V_A/\Omega$
- Growth rate $\omega^2 = \Omega^2 - k^2 V_A^2$
 - Instability happens over rotation time scale of disk for long wavelengths
 - $\omega \sim 10 * \Omega$ (S. M. O'Neil et al. ApJ, 2011)

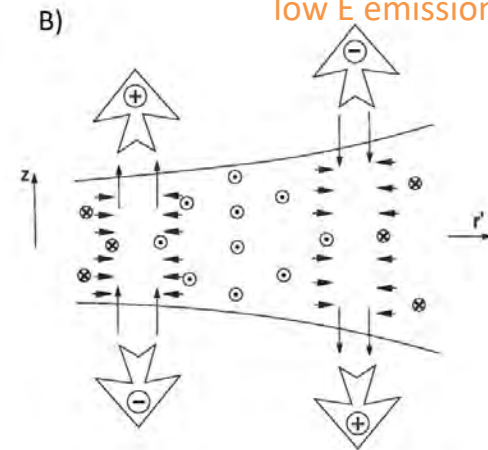
High State (Soft State)



Low State (Hard State)

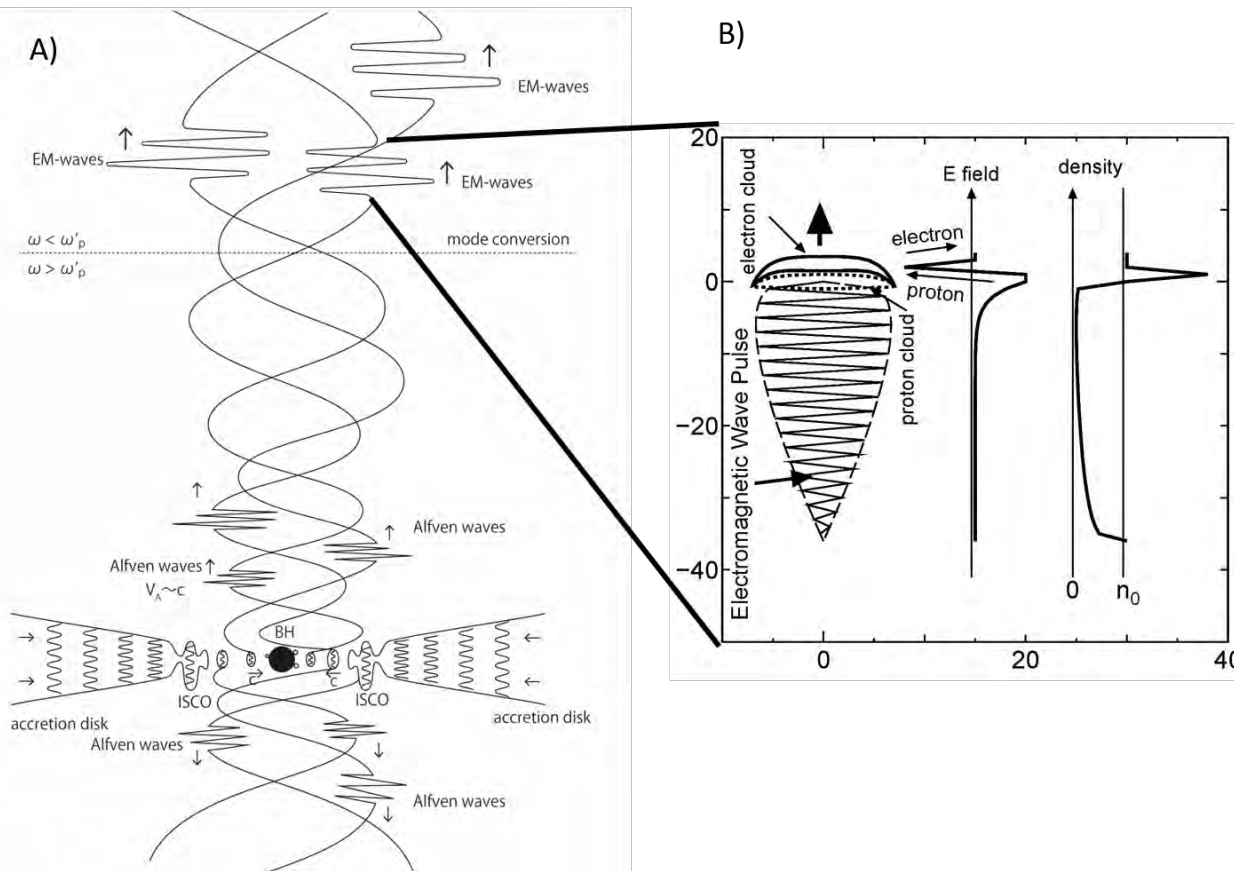


Halo heating and acceleration
low E emissions



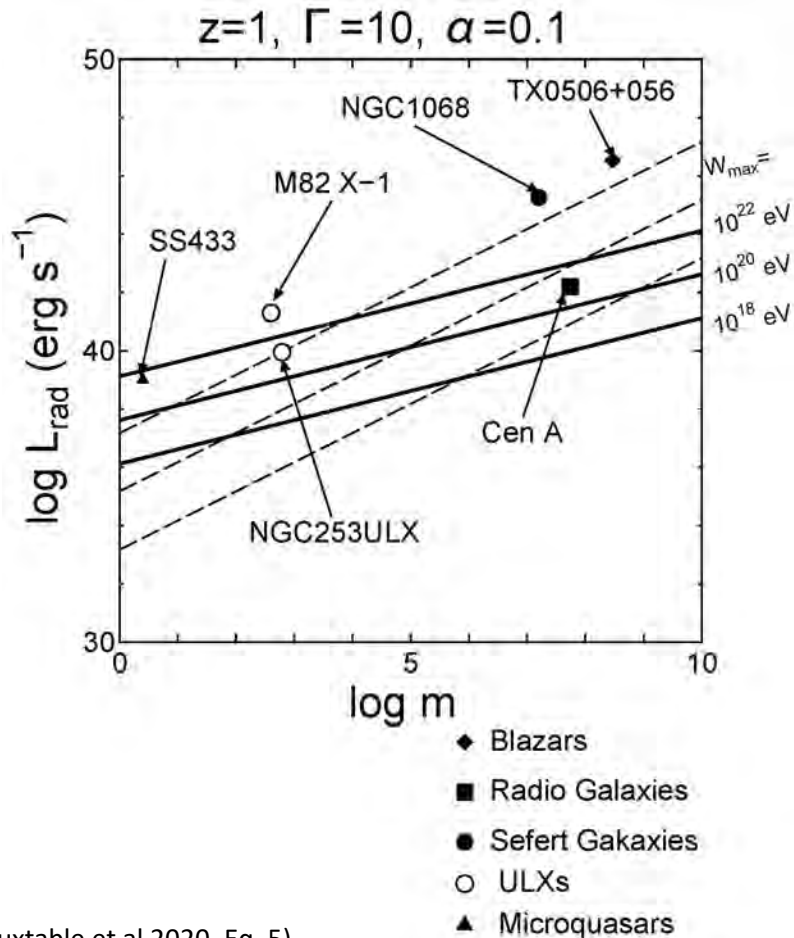
WFA in Jets

Plasma at the base of the jet is in the over-dense state $\omega < \omega_p, \omega_c$. Eruptive accretions create Alfvén waves in the base of the jet. Intense Alfvén waves eventually become intense EM waves as $\omega_p \rightarrow \omega$, and $V_A \rightarrow c$.



$a_0 \approx 10^{6-10}$ (extremely high compared to laboratory plasmas)
 $n_e \approx 10^4$ (near BH); 10^1 cm^{-3} (along jet, away from BH)
 $D \approx 10^{11-19} \text{ cm}$ (acceleration length)

WFA Generating UHE Emissions



(Huxtable et al 2020, Eq. 5)

$$W_{\text{max}} = \frac{1}{9} \left(\frac{e^4 c^2 R_0^2}{2m_e e^4 \kappa_T^2} \right)^{1/3} z \Gamma \alpha^{2/3} \dot{m}^{4/3} m^{2/3}$$

- Pondermotive force, $F = \Gamma m_e c a \omega_A$
- Acceleration length, $D = ca/\omega_A$
- The extremely large a_0 in these jets allows for the acceleration of protons, not just electrons
- Can expect to observe UHECRs from all central masses that possess an accretion disk and jets. The validity of WFA is bolstered by this as it is unifying for the explanation of AGNs

Formula's

- Given L_{rad} (typically estimated from x-ray observations) and m (typically from QPO/stellar dynamics), as well as assuming typical values for a couple parameters (such as the conversion efficiency, α)
- We can derive the “Quantities” circled

Table 1. Time Scales, Maximum Energy, and Luminosities predicted by Tajima et al. (2020)

Quantities	Scaling Laws	Units	Equation Numbers
$2\pi/\omega$	$8.2 \times 10^{-5} \alpha^{-1/2} \dot{m} m$	s	2
$1/\nu$	$7.3 \times 10^{-5} \alpha^{-1/2} m$	s	3
D_3/c	$1.7 \times 10^2 \alpha^{5/6} \dot{m}^{5/3} m^{4/3}$	s	4
W_{max}	$3.2 \times 10^{-31} z \Gamma \alpha^{2/3} m^{-2/3} L_{rad}^{4/3}$	eV	5
L_{rad}	$1.5 \times 10^{38} \dot{m} m$	erg s ⁻¹	1
L_γ	$2.78 \sigma \alpha^{1/2} L_{rad}$	erg s ⁻¹	8
$LUHECR$	$2.78 \sigma \zeta \alpha^{1/2} L_{rad}$	erg s ⁻¹	9

(Huxtable et al 2020, Eq. 5)

Results

Table 2. Comparison of observed parameters (shaded) and theoretical parameters (without shade), where [log here is log base 10](#). Theoretical and observational values for a range of astrophysical objects, including a blazar (BL), a radio galaxy (RG), a Seyfert galaxy (SyG), starburst galaxies (SBG) and a micro-quasar (MQ).

parameter	TX 0506+056	Cen A	NGC1068	M82	NGC 0253	SS 433
type	BL	RG	SyG	SBG	SBG	MQ
$\log d$ (pc)	9.24	6.53	7.15	6.56	6.54	3.54
$\log M_{\text{BH}}(M_{\odot})$	8.48	7.74	6.20	2.60	2.79	0.40
$\log L_{\text{rad}}(\text{erg s}^{-1})$	45.23	42.36	45.26	41.30	39.96	40.00
$\log W_{\text{max}}$ (eV)	24.49	21.16	26.05	23.17	21.26	22.91
$\log L_{\text{UHECR}}(\text{erg s}^{-1})$	43.17	40.31	43.20	39.24	37.90	37.94
$F_{\text{UHECR}}(/100 \text{ km}^2/\text{yr})$	-	0.69	-	0.052	0.0026	-
$F_{\text{UHECR}}(/100 \text{ km}^2/\text{yr})$	-	0.016	-	0.04	0.013	-
$\log 2\pi/\omega$ (s)	3.47	0.62	3.50	-0.46	-1.81	-1.76
$\log 2\pi/\omega$ (s)	< 4.68	-	-	-	-	-
$\log 1/\nu$ (s)	4.84	4.10	2.56	-1.04	-0.85	-3.24
$\log 1/\nu$, (s)	< 6.38	4.18	-	-0.70	< 2.0	< 1.0
$\log L_{\gamma}(\text{erg s}^{-1})$	44.17	41.31	44.20	40.24	38.90	38.94
$\log L_{\gamma}(\text{erg s}^{-1})$	47.08	38.04	45.53	40.18	39.78	37.57

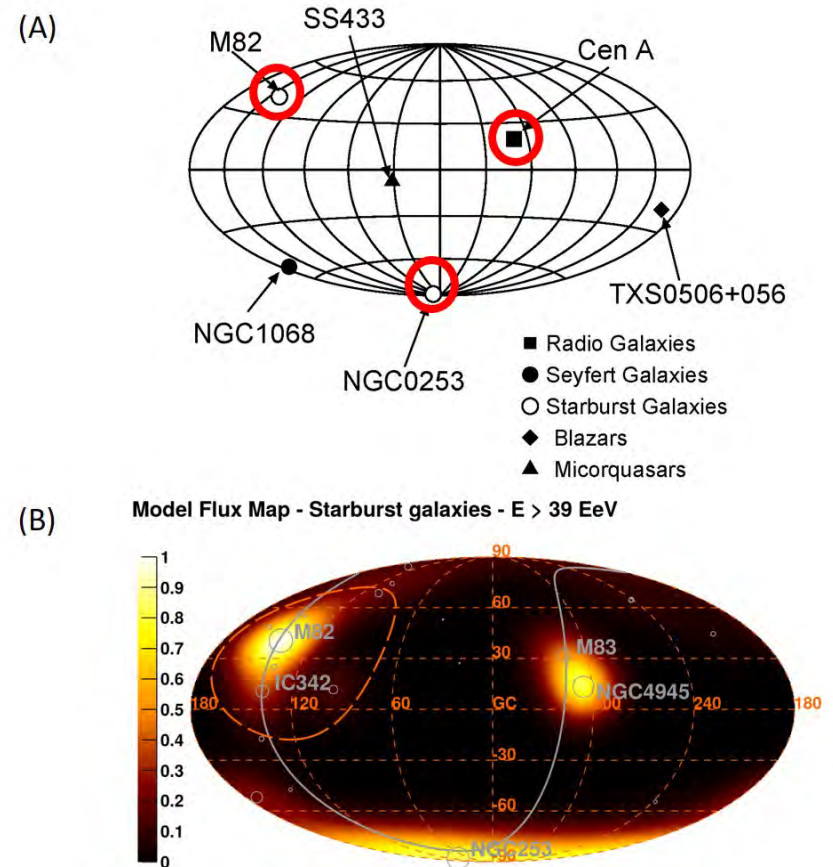
(Huxtable et al 2020, Eq. 5)

Jet Spreading Effects

- The previous work does not take into account fine tuning of the jet spreading parameter, p , which describes the jet's radius, $b(D) = R_0 m \left(\frac{D}{R_0 m} \right)^p$
 - $p \sim 0.5$ in the case of M87, the closest AGN to us
 - Alters W_{max} and acceleration length, D_3 (as well as ω'_c and ω'_p layers too)
- Both the B field and density decrease along the length of the jet. The inhomogeneity introduces mode conversion
 - Originally an Alfvén wave, the pulse transits many resonance and cutoff layers and thus converts many times before eventually becoming an EM pulse
 - Conversely, an EM wave (such as radio) incident upon a plasma can penetrate and convert into a different wave if resonance/cutoff layers exist beneath the plasma surface

Localization (Spatial Structure/Anisotropy)

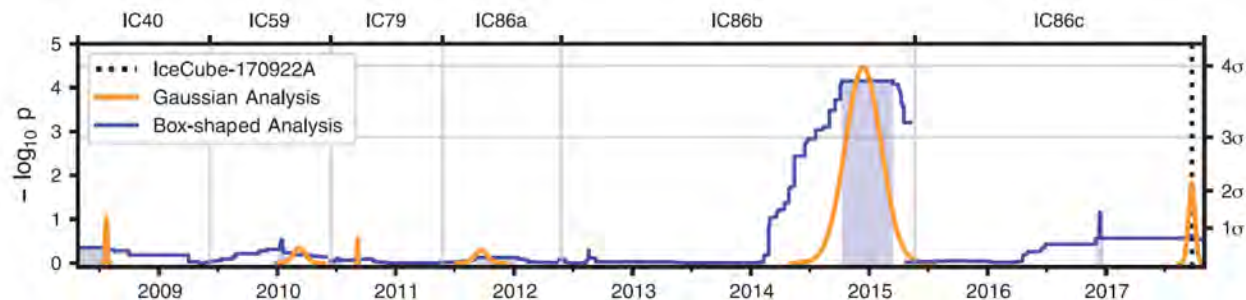
- WFA, since it accelerates particles in a linear fashion, would naturally lead to localized “hotspots” of UHECR, UHE gamma-ray, and neutrino emission
- Fermi acceleration predicts a nearly uniform 4π concentration of these signals in the skymap



Burst in Emission (Temporal Structure)

- Time structure: simultaneous arrival of neutrino with other signal
 - Chance coincidence of the neutrino with the flare of TXS 0506+056 is disfavored at the 3σ level in any scenario where neutrino production is linearly correlated with gamma-ray production or with gamma-ray flux variations.
- Coincidence of neutrino location with blazar
- Periodic observation of neutrino burst (fig. ref. [2])
- Good candidate for UHECRs

Neutrino data from TXS 0506+056 fitted with gaussian, and box-shaped profiles. Gaussian is colocated with 2018 burst



IceCube Collab. Science (2018)

Anti-Correlation Between Flux & Index

- Anti-correlation b/w flux and index
 - After sudden accretions (increase in flux), the accretion disk “relaxes” back to the low beta state (low index ~ 2)
 - Then the magnetic field begins to amplify again, high beta state (index >2), and the flux drops off until MRI takes over again
- WFA explains corresponding increases in luminosity and decreases in spectral index.
- Again, Fermi acceleration is totally unrelated to this, however, this is mostly a disk phenomenon

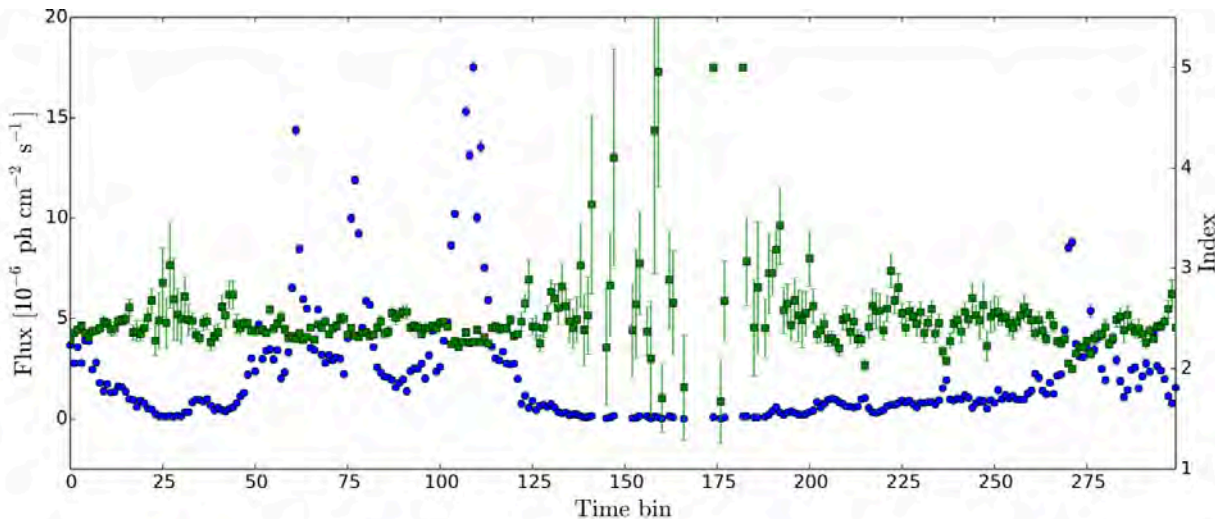


Figure 4. Shown are the flux (blue circles, left-hand axis) and spectral index (green squares, right-hand axis) for 3C 454.3 in 300 time bins of 7.9 d duration. An anticorrelation can be seen: the peaks in flux correspond to dips in the spectral index and vice versa.

Summary

- Simple yet encompassing picture that describes a large amount of phenomenon
 - Hope to shed light on understanding of the existence of UHECRs, neutrinos and gamma-rays bursts from AGNs
- Hopeful for future observations/experiments
 - detecting spatially resolved UHECRs to further test the theory
 - Refine characteristic values (such as mass, total luminosities, etc) for each object